Communications in Nonlinear Science and Numerical Simulation 119 (2023) 107097

Contents lists available at ScienceDirect

Communications in Nonlinear Science and Numerical Simulation

journal homepage: www.elsevier.com/locate/cnsns

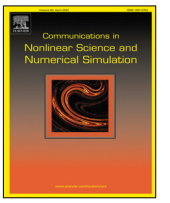

Research paper

Probabilistic analysis of a general class of nonlinear random differential equations with state-dependent impulsive terms via probability density functions

Vicente J. Bevia [a], Juan C. Cortés [a,*], Marc Jornet [b], Rafael J. Villanueva [a]

[a] Instituto Universitario de Matemática Multidisciplinar, Universitat Politècnica de València, 46022 Valencia, Spain
[b] Departament de Matemàtiques, Universitat de València, 46100 Burjassot, Spain

ARTICLE INFO

Article history:
Received 9 July 2022
Received in revised form 15 November 2022
Accepted 29 November 2022
Available online 7 January 2023

MSC:
2010
34A34
34F05
92D25

Keywords:
Random differential equations
Dirac-delta impulse terms
First probability density function
Liouville–Gibbs equation
Random variable transformation technique

ABSTRACT

In this contribution, we rigorously construct a pathwise solution to a general scalar random differential equation with state-dependent Dirac-delta impulse terms at a finite number of time instants. Furthermore, we obtain the first probability density function of the solution by combining two main results, firstly, the Liouville–Gibbs equation between the impulse instants, and secondly, the Random Variable Transformation technique at the impulse times. Finally, all theoretical findings are illustrated on two stochastic models, widely used in mathematical modeling, carrying on computational simulations.

1. Introduction

Differential equations-based dynamical systems, also known as continuous dynamical systems, have become the cornerstone of the modeling of real-world phenomena. This key role played by dynamical systems includes theoretical analysis and simulations of physical systems in engineering, biology, medicine, etc.

Most naturally occurring phenomena can be described as a function with a continuous rate of change with respect to time. However, there are cases where the system suddenly changes its state, affecting its dynamics in ways that require special mathematical tools for correctly modeling its dynamics. For example, when determining the effect of a pesticide applied to an insect infestation at a specific time, the insect population could be suddenly reduced. As a consequence, the function describing the population density of insects with respect to time would be discontinuous at that time instant. Similar situations appear when modeling the time evolution of a tumor mass under the effect of certain therapies, such as partial tumor removal at specific times instants. The appropriate modeling of this kind of problem may help doctors simulate the future evolution of the tumor mass in multiple scenarios. These are known as harvesting models and are primarily used to analyze possible control strategies [1–3].

* Corresponding author.
E-mail address: vibees@upv.es (J.C. Cortés).

https://doi.org/10.1016/j.cnsns.2023.107097

Dynamical systems consist of an input, a set of parameters, and an output. When analyzing and predicting the behavior of a real-world system, one must obtain a set of measurements with the objective of calibrating the model parameters so that the dynamical system output closely resembles the measurement data. However, it is practically impossible to have a perfect fit between the model output and the measurements. The reason behind this impossibility can be classified into two categories [4,5]:

- Mathematical models are usually simplifications of real-world systems, leaving out some variables that, unawarely, may affect the evolution of the system. This is usually termed as *epistemic, or structural uncertainty*.
- Measurement devices have error tolerances which imply that, whatever measurement has been taken to obtain a given parameter or initial condition, one must consider a given amount of uncertainty. Also, some models include variables that cannot be directly measured or that present a high variability. These facts entail that the information given by the mathematical model must also account for uncertainty in model parameters (initial/boundary conditions, source term and/or coefficients). This is usually termed *aleatoric uncertainty*.

Therefore, to have a truly accurate and realistic model of a real-world system, one has to quantify all the uncertainties appearing in the model. One of the most flexible approaches used for the Uncertainty Quantification (UQ) of continuous dynamical systems is to consider Random Differential Equations (RDEs) [5–7].

In the setting of RDEs, the inputs of the equation (initial/boundary conditions, forcing term and/or coefficients) are assumed to be random variables and/or stochastic processes defined on a probability space $(\Omega, \mathcal{F}, \mathbb{P})$. Apart from rigorously obtaining the solution of the RDE, which is a stochastic process, say $X(t) \equiv X(t, \omega)$, $\omega \in \Omega$, many contributions also focus on computing the mean and variance functions since they provide statistical relevant information of the output. However, the greatest goal is to determine the so called n-dimensional Probability Distribution Function, also termed n-PDFs or *n-fidis* [7], and particularly, the 1-PDF of the solution. This deterministic function, say $f_{X(t)}(x)$ (often also denoted by $f(x, t)$), allows the computation of any statistical one-dimensional moment,

$$\mathbb{E}[(X(t, \omega))^k] = \int_{-\infty}^{\infty} x^k f_{X(t)}(x)\mathrm{d}x, \quad k = 1, 2, \ldots,$$

here $\mathbb{E}[\ ]$ denotes the expectation operator. The 1-PDF also permits computing the probability that the solution lies within any interval of interest

$$\mathbb{P}[\{\omega \in \Omega : a \leq X(t, \omega) \leq b\}] = \int_a^b f_{X(t)}(x)\mathrm{d}x,$$

as well as the computation of confidence intervals.

In the setting of RDEs, the task of obtaining the 1-PDF of a stochastic process has been classically done in two main ways, firstly, via Monte-Carlo sampling and, secondly, by applying the Random Variable Transformation (RVT) technique. On the one hand, obtaining the 1-PDF at a certain time instant via Monte-Carlo sampling consists in numerically obtaining samples of the random variables appearing in the RDE and then simulating their evolution up to the corresponding time in order to build the histogram that represents the 1-PDF at the desired time [8]. Although this method is widely used and is fairly simple to implement in its naive version, it is also true that a vast number of samples must be used to obtain an accurate representation of the PDF [9,10]. Nevertheless, improved Monte-Carlo techniques, such as variance-reduction, multi-level, etc., have been successfully designed to speed up the raw Monte-Carlo method [11]. On the other hand, the RVT technique gives a closed formula of the 1-PDF at any time instant. Although this method provides great insight into the dynamics of the solution of the problem, it relies on the exact knowledge of the solution of the corresponding RDE [12,13], which is often not the case, as it is well-known.

In connection with what we have done in our previous works [14–16], we are going to make use of a theorem that links the 1-PDF of a RDE solution to the solutions of a certain deterministic Partial Differential Equation (PDE). In particular, it is linked with the Continuity [17,18], Liouville [19–21] or Liouville–Gibbs [7] equation. This result gives a closed-form solution of the 1-PDF, when available, as well as the chance to study its qualitative dynamical behavior over time. Also, the specific form of the PDE allows the use of several accurate and efficient deterministic numerical methods when a closed-form solution of the PDE is not available.

This contribution is organized as follows. Section 2 is divided into two parts; in Section 2.1, we rigorously build a pathwise solution of an RDE with state-dependent impulse terms under mild hypotheses on the scalar field. Then, in Section 2.2, we apply the Liouville–Gibbs equation to obtain the corresponding 1-PDF of the solution of the RDE. We will make particular emphasis on the determination of the 1-PDF behavior at the interface of the discontinuities due to the application of the impulses. We will do so without any knowledge of the explicit form of the field function of the RDE. This results in the application of the Liouville–Gibbs approach to general RDEs. To illustrate this latter fact, in Section 3, we apply the theoretical findings to devise a computational procedure that will be applied to two relevant models widely used in biology and medicine. Conclusions are drawn in Section 4.

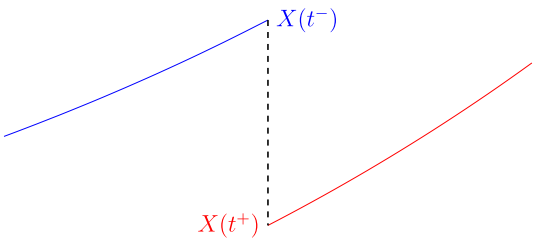

Fig. 1. Path solution to (2.1) in a neighborhood of an impulse time. Conditions (1)–(3) are clearly reflected in this example.

2. Theory

In this section we will study, from a probabilistic standpoint, the following random Initial Value Problem (IVP):

$$\begin{cases} \dfrac{\mathrm{d}X(t,\omega)}{\mathrm{d}t} &= g(X(t,\omega),t,\mathbf{A}(\omega)) - \displaystyle\sum_{k=1}^{N} \Gamma_k(\omega)\delta(t-t_k)X(t,\omega), \quad t > t_0, \\ X(t_0,\omega) &= X_0(\omega). \end{cases} \tag{2.1}$$

Here t_0 denotes a real number; $X_0(\omega)$, $\mathbf{A}(\omega) := (A_1(\omega),\ldots,A_m(\omega))$ and $\{\Gamma_k(\omega)\}_{k=1}^N$ are assumed to be independent absolutely continuous random variables defined on the Hilbert space $\mathrm{L}^2(\Omega,\mathbb{R})$, whose elements are real-valued random variables with finite variance and $(\Omega,\mathcal{F},\mathbb{P})$ denotes a complete probability space [22]; $\delta(t-t_k)$ stands for the Dirac delta function [23] acting at the prefixed time instants $t=t_k$, $k=1,\ldots,N$ and g is known as the *(scalar) field function* satisfying certain conditions that will be specified later. Finally, $X(t,\omega)$ denotes the solution of the random IVP (2.1). For the sake of simplification in the notation, hereinafter, the ω-dependence will be hidden in the notation when convenient.

Observe that we set the impulse terms with the negative sign because, in most practical cases, one is interested in the instantaneous change of the system state in a way that is opposite to its unaltered dynamics. For example, when modeling tumor growth, one is often interested in the dynamics after the instantaneous retrieval of a part of the tumor. Alternatively, when modeling the decay of drug concentration in a person's bloodstream, interest is shifted to simulating the concentration after the drug administration. In the setting of these two illustrative examples, the dynamics before the retrieval of the tumor or drug administration is governed by the specified form of the field function g.

Regarding the regularity assumptions on g, they will be determined by the sample realizations of the parameter random vector $\mathbf{A}(\omega)$. Therefore, we consider the following random events:

$$E_1 = \{\omega\in\Omega : g(\cdot,t,\mathbf{A}(\omega)) \in \mathrm{Lip}(\mathbb{R}), \text{ uniformly in } t\}, \tag{2.2}$$

$$E_2 = \{\omega\in\Omega : g(x,\cdot,\mathbf{A}(\omega)) \in C^0([t_0,\infty)) \text{ for all } x\geq 0\}, \tag{2.3}$$

and assume that both sets are $\mathbb{P}-$measurable, with $\mathbb{P}[E_1\cap E_2]=1$. The solution of the random IVP (2.1) is a stochastic process, which can be seen as a family of deterministic trajectories, or paths, indexed in the underlying probability space Ω; that is, $\{X([t_0,+\infty,]\omega)\}_{\omega\in\Omega}$. Therefore, by fixing $\omega\in\tilde{\Omega} := E_1\cap E_2$ we can analyze a random trajectory of the IVP (2.1) using the deterministic theory of ODEs [24].

The sample-fixed ODE defining (2.1) does not verify the hypotheses of either the Cauchy–Peano [25], or the Picard–Lindelöf theorems [24]. Therefore, a *priori*, we cannot guarantee the existence of a solution or its uniqueness. However, the regularity assumptions given by conditions (2.2) and (2.3) are sufficient for the global existence of each sample trajectory. Therefore, if a solution $X(t)$ exists, it must be "well-behaved" between the impulse times $\{t_k\}_{k=1}^N$. In particular, this behavior implies the following conditions (see Fig. 1):

(1) Continuous differentiability in (t_{k-1},t_k), $k=1,\ldots,N$.
(2) Existence and finiteness of $X(t_k^+) := \lim_{t\to t_k^+} X(t)$ for all $k=0,\ldots,N$ and $X(t_k^-) := \lim_{t\to t_k^-} X(t)$ for $k=1,\ldots,N$.
(3) Uniqueness of the solution in (t_{k-1},t_k) given $X(t_{k-1}^+)$, $X(t_k^-)$ or some $X(t^*)$, with $t^*\in(t_{k-1},t_k)$, for $k=1,\ldots,N$.

2.1. Pathwise (weak) solution

Keeping the comments in the previous paragraphs in mind, we will build a pathwise solution for the random IVP (2.1). Let us fix $\omega\in\tilde{\Omega}$ and compute the deterministic Laplace transform [26] to the corresponding IVP (2.1). Denoting $\lambda(s)=\mathcal{L}[X(\cdot,\omega)](s)$, $x_0=X_0(\omega)$, $\mathbf{a}=\mathbf{A}(\omega)$ and, momentarily, dropping the ω notation, we obtain

$$s\lambda(s) - x_0 = \mathcal{L}[g(X(\cdot),\cdot,\mathbf{a})](s) - \sum_{k=1}^{N} \Gamma_k \mathrm{e}^{-st_k} X(t_k),$$

$$\lambda(s) = \frac{x_0}{s} + \frac{\mathcal{L}[g(X(\cdot), \cdot, \mathbf{a})](s)}{s} - \sum_{k=1}^{N} \Gamma_k \frac{e^{-st_k}}{s} X(t_k). \tag{2.4}$$

Computing the inverse Laplace transform of (2.4) gives

$$X(t) = x_0 + \int_{t_0}^{t} g(X(s), s, \mathbf{a})ds - \sum_{k=1}^{N} \Gamma_k X(t_k) H(t - t_k), \tag{2.5}$$

where $H(\cdot)$ is the Heaviside function, defined as

$$H(x) = \begin{cases} 1 & x \geq 0, \\ 0 & x < 0. \end{cases}$$

Notice that expression (2.5) is actually the integral form of Eq. (2.1), where $\delta(\cdot)$ acts as a measure [27]. We can now see what happens at the first impulse. The value of $X(t_1)$ is, a *priori*, unknown. However, substituting $t = t_1$ and solving for $X(t_1)$, (2.5) yields

$$X(t_1) = \frac{x_0 + \int_{t_0}^{t_1} g(X(s), s, \mathbf{a})ds}{1 + \Gamma_1} = \frac{\lim_{t \to t_1^-} X(t)}{1 + \Gamma_1} := \frac{X(t_1^-)}{1 + \Gamma_1}. \tag{2.6}$$

Let us emphasize the interesting transformations given by the previous equation. Consider an arbitrary but fixed ω. We have the following transformations:

(1) The transformation will be well-defined (and invertible) if $\Gamma_1(\omega) \neq -1$.
(2) If $\Gamma_1(\omega) = 0$, the identity transformation applies; that is, $X(t_1, \omega) = X(t_1^-, \omega)$.
(3) If $\Gamma_1(\omega) \in (0, \infty)$, we will have $X(t_1, \omega) < X(t_1^-, \omega)$.
(4) If $\Gamma_1(\omega) \in (-1, 0)$, we will have $X(t_1, \omega) > X(t_1^-, \omega)$.
(5) If $\Gamma_1(\omega) \in (-2, -1)$, we will have $X(t_1, \omega) < -X(t_1^-, \omega)$.
(6) If $\Gamma_1(\omega) \in (-\infty, -2)$, we will have $X(t_1, \omega) > -X(t_1^-, \omega)$.

Note that condition (1) occurs almost surely (i.e., with unit probability) when Γ_1 is an absolutely continuous random variable.

Now, let us see what happens after the impulse. From (2.5) and the previous relation for $X(t_1)$, we can compute the jump induced in the paths by the impulse term

$$X(t_1^+) - X(t_1^-) = \int_{t_1^-}^{t_1^+} g(X(s), s, \mathbf{a})ds - \Gamma_1 X(t_1). \tag{2.7}$$

Let us see that the integral term in the previous equation is 0,

$$\left| \int_{t_1^-}^{t_1^+} g(X(s), s, \mathbf{a})ds \right| \leq \lim_{\varepsilon \to 0} \left(\int_{t_1 - \varepsilon}^{t_1} |g(X(s), s, \mathbf{a})|ds + \int_{t_1}^{t_1 + \varepsilon} |g(X(s), s, \mathbf{a})|ds \right) \tag{2.8}$$

$$\leq \lim_{\varepsilon \to 0} \left(\sup_{t \in [t_1 - \varepsilon, t_1)} |g(X(t), t, \mathbf{a})|\varepsilon + \sup_{t \in (t_1, t_1 + \varepsilon]} |g(X(t), t, \mathbf{a})|\varepsilon \right) \tag{2.9}$$

$$= 0,$$

because both supremum terms are finite. This is due to the three conditions (1)–(3) stated before the current subsection. Using (2.6), equality (2.7) now reads,

$$X(t_1^+) - X(t_1^-) = -\Gamma_1 X(t_1) \iff X(t_1^+) = \frac{X(t_1^-)}{1 + \Gamma_1} = X(t_1).$$

That is, the general solution (2.5) is right-continuous at the first impulse. Furthermore, notice that (2.7) and (2.9) show that right-continuity at impulse times must be verified by solutions of Eq. (2.1). Recovering the ω-notation, the previous identity is stated as

$$X(t_1, \omega) = X(t_1^+, \omega) = \frac{X(t_1^-, \omega)}{1 + \Gamma_1(\omega)}, \tag{2.10}$$

which means that, for every sample $\omega \in \tilde{\Omega}$, the paths are right-continuous at $t = t_1$. We can follow the same procedure for the following impulse times. For example, for all $t \in [t_1, t_3)$, the solution process is given by

$$X(t) = x_0 + \int_{t_0}^{t} g(X(s), s, \mathbf{a})ds - \Gamma_1 X(t_1) - \Gamma_2 X(t_2) \mathrm{H}(t - t_2). \tag{2.11}$$

Now, by using (2.5), we see that, at time $t = t_2$, (2.11) can be written as:

$$X(t_2) = X(t_1) + \int_{t_1}^{t_2} g(X(s), s, \mathbf{a})\mathrm{d}s - \Gamma_2 X(t_2), \tag{2.12}$$

which yields

$$X(t_2) = \frac{X(t_1) + \int_{t_1}^{t_2} g(X(s), s, \mathbf{a})\mathrm{d}s}{1+\Gamma_2} = \lim_{t\to t_2^-} \frac{X(t)}{1+\Gamma_2} := \frac{X(t_2^-)}{1+\Gamma_2}. \tag{2.13}$$

Following the same reasoning as in (2.7) and (2.8)–(2.9), the value after the impulse will be

$$X(t_2^+) - X(t_2^-) = -\Gamma_2 X(t_2) = -\frac{\Gamma_2}{1+\Gamma_2} X(t_2^-) \iff X(t_2^+) = \frac{X(t_2^-)}{1+\Gamma_2}. \tag{2.14}$$

The steps followed for the analysis of the first and second impulse times can be easily generalized for any number of finite impulse times. Particularly, at a given impulse time t_k, and recovering the ω-notation:

$$X(t_k^+, \omega) = X(t_k, \omega) = \frac{X(t_k^-, \omega)}{1+\Gamma_k(\omega)}, \tag{2.15}$$

for all $k = 1, \ldots, N$. Also, note that the transformation properties for the first impulse, that are listed in (1)–(6) after Eq. (2.6), apply at every impulse time and for every impulse term.

Summarizing, we have constructed a right-continuous pathwise solution of the random IVP (2.1), given by

$$X(t, \omega) = X_0(\omega) + \int_{t_0}^{t} g(X(s, \omega), s, \mathbf{A}(\omega))\mathrm{d}s - \sum_{k=1}^{N} \Gamma_k(\omega) X(t_k, \omega)\mathrm{H}(t - t_k), \quad t \geq t_0, \tag{2.16}$$

$$X(t_k, \omega) = \frac{X(t_k^-, \omega)}{1+\Gamma_k(\omega)} = X(t_k^+, \omega), \quad \omega \in \tilde{\Omega}. \tag{2.17}$$

Note that, if we can assure $\{X([t_0, \infty], \omega)\}_{\omega\in\tilde{\Omega}} \subseteq \mathcal{D}$, for some set $\mathcal{D}$ (independently of the realizations ω), then the Lipschitz regularity of g can be simplified to the set $\mathcal{D}$; that is, we would only need Lipschitz regularity of g in the set $\mathcal{D}$.

2.2. Probability density function evolution

Because of the local (and global) probability conservation property of RDEs, whose field function we denote by b, we can obtain an evolution PDE which is verified by its 1-PDF. The theorem can be stated as follows

Theorem 2.1 ([15]). *Let $b(\cdot, t) : \mathbb{R} \longrightarrow \mathbb{R}$ be a Lipschitz-continuous function for all $t \in (t_0, \infty)$, and continuous in t. Let $X(t, \omega)$, $t \geq t_0$, $\omega \in \Omega$ be the stochastic process verifying the following RDE in the almost-surely or mean square sense:*

$$\begin{cases} \dfrac{\mathrm{d}X(t)}{\mathrm{d}t} = b(X(t), t), \quad t > t_0, \\ X(t_0) = X_0 \in \mathrm{L}^2(\Omega, \mathbb{R}). \end{cases} \tag{2.18}$$

Let $\mathcal{D}$ be a set such that $\{X([t_0, \infty], \omega)\}_{\omega\in\Omega} \subset \mathcal{D}$. Then, the 1-PDF of the stochastic process $X(t)$, denoted by $f = f_{X(t)}$, verifies the Liouville PDE:

$$\begin{cases} \partial_t f(x, t) + \partial_x[bf](x, t) = 0, \quad x \in \mathcal{D}, \quad t > t_0, \\ f(x, t_0) = f_0(x), \quad x \in \mathcal{D}, \\ \partial_x f(x, t) = 0, \quad x \in \partial\mathcal{D}, \quad t \geq t_0, \end{cases} \tag{2.19}$$

where f_0 is the PDF of $X_0 = X_0(\omega)$.

The boundary condition $\partial_x f(x, t) = 0$ appears naturally from the probability conservation property of RDEs when the phase space is bounded (otherwise, the PDF will decay to 0 naturally). It is the mathematical form of saying that no probability exits or enters the phase space at its boundaries (see [7, Th. 6.2.2] and [17, Sec. 4.1.2]). However, in most one-dimensional models, such as the ones that will be analyzed in Section 3, this condition is automatically verified because of the form of its field function [14,15]. In higher dimensions, this condition may have to be explicitly stated [16].

When the RDE has random parameters, IVP (2.19) becomes a family of deterministic PDE problems indexed in the realizations, $\mathbf{a}$, of the random parameter vector, $\mathbf{A} = \mathbf{A}(\omega)$,

$$\begin{cases} \partial_t f(x, t \mid \mathbf{a}) + \partial_x[b(x, t, \mathbf{a}) f(x, t \mid \mathbf{a})] = 0, \quad x \in \mathcal{D} \subseteq \mathbb{R}, \quad t > t_0, \\ f(x, t_0 \mid \mathbf{a}) = f_0(x), \quad x \in \mathcal{D}. \end{cases} \tag{2.20}$$

The PDF of the RDE solution (independent of parameter realizations) is obtained by marginalizing the joint PDF of both the solution and the parameter vector $\mathbf{A}$, which, using the conditional PDF, can be written as:

$$f(x,t)=\int_{\mathbb{R}^m} f(x,t\mid \mathbf{a})f_{\mathbf{A}}(\mathbf{a})\mathrm{d}\mathbf{a}=\mathbb{E}_{\mathbf{A}}[f(x,t\mid \mathbf{A})], \tag{2.21}$$

where $f_{\mathbf{A}}$ is the parameters' joint PDF and $\mathbb{E}_{\mathbf{A}}$ denotes the expectation operator with respect to the random vector $\mathbf{A}$. This shows that the PDF can be obtained by solving (2.20) for all realizations $\mathbf{a}$ of $\mathbf{A}$ and then computing its mean.

However, a *priori* we can only assure the global-in-time existence of a solution to the Liouville equation when the field function $b(\cdot,t)$ is Lipschitz continuous, uniformly in t. As mentioned earlier, the field under consideration, $b(x,t)=g(x,t)-\sum_k \gamma_k\delta(t-t_k)x$, does not verify this hypothesis at the impulse times $\{t_k\}_{k=1}^N$. Our objective is to obtain a condition such as the jump condition (2.7) for the PDF. This will allow the computation of the evolution of f_0, accurately capturing the discontinuities at the impulse times.

2.2.1. PDF transformation at the impulse times

Let us turn back to the set of conditions in (2.17), which are identities between random variables. We are going to make use of the RVT theorem, which can be written as follows:

Theorem 2.2 (*[7,14]*). *Let $\mathbf{X}$, $\mathbf{Y}:\Omega\to\mathbb{R}^M$ be two random vectors with PDFs $f_{\mathbf{X}}$ and $f_{\mathbf{Y}}$, respectively. Assume that there is a one-to-one, C^1 function $\mathbf{h}$ such that $\mathbf{X}=\mathbf{h}(\mathbf{Y})$. Then, denoting $\mathbf{h}^{-1}$ as the inverse mapping of $\mathbf{h}$,*

$$f_{\mathbf{X}}(\mathbf{x})=f_{\mathbf{Y}}(\mathbf{h}^{-1}(\mathbf{x}))\left|\frac{\partial\mathbf{h}^{-1}(\mathbf{x})}{\partial\mathbf{x}}\right|, \tag{2.22}$$

where $\left|\frac{\partial\mathbf{h}^{-1}(\mathbf{x})}{\partial\mathbf{x}}\right|$ denotes the absolute value of the determinant of the Jacobian matrix.

As in the case of the pathwise solution analysis, let us consider the first transformation in detail and then we will write the result for the general case. Let $f(\cdot,t_1)$ be the PDF of the stochastic process solution at a given impulse time t_1; that is, the PDF of $X(t_1,\cdot)$ (which is unknown). Let $f(\cdot,t_1^-)$ be the PDF before the jump; that is, the PDF of $X(t_1^-,\cdot)$ (which is known because it verifies the Liouville equation in (t_0,t_1)). Using (2.10) we can compute the Jacobian of the variable transformation:

$$X(t_1,\omega)(1+\Gamma_1(\omega))=X(t_1^-,\omega)\iff |J|=\left|\frac{\partial X(t_1^-,\omega)}{\partial X(t_1,\omega)}\right|=|1+\Gamma_1(\omega)|. \tag{2.23}$$

Denoting the joint PDFs of $X(t,\cdot)$ and Γ_1 by $f_{(X(t),\Gamma_1)}$, for $t=t_1,\ t_1^-$, the application of the RVT theorem leads to

$$f_{(X(t_1),\Gamma_1)}(x,\gamma_1,t_1)=f_{(X(t_1^-),\Gamma_1)}\left(x(1+\gamma_1),\gamma_1,t_1^-\right)|1+\gamma_1|=f\left(x(1+\gamma_1),t_1^-\right)f_{\Gamma_1}(\gamma_1)|1+\gamma_1|,$$

because $X(t_1^-,\cdot)$ is independent from Γ_1, which only appears at the impulse time. Finally, to obtain the PDF of $X(t_1,\cdot)$, we have to marginalize respect to Γ_1

$$f(x,t_1)=\int_{\mathcal{D}(\Gamma_1)} f\left(x(1+\gamma_1),t_1^-\right)|1+\gamma_1|f_{\Gamma_1}(\gamma_1)\mathrm{d}\gamma_1=\mathbb{E}_{\Gamma_1}[f\left(x(1+\Gamma_1),t_1^-\right)|1+\Gamma_1|], \tag{2.24}$$

for all $x>0$, which shows that, at the jump, there is a rescaling of $f(\cdot,t_1^-)$, both in its argument and in its value, for every realization of Γ_1 (see Fig. 2). The average of these transformations gives the PDF of $X(t_1,\cdot)$. Note that, in (2.24), $\mathcal{D}(\Gamma_1)$ denotes the domain of random variable $\Gamma_1(\omega)$.

Now, the Liouville equation describes the evolution of the PDF (2.24) until the following impulse time t_2. Clearly, at any other impulse time, we will have the same case as for t_1:

$$f(x,t_k)=\mathbb{E}_{\Gamma_k}[f\left(x(1+\Gamma_k),t_k^-\right)|1+\Gamma_k|],\quad \forall x>0,\quad k=1,\dots,N, \tag{2.25}$$

because of the relations at (2.17).

2.2.2. Evolution between impulse times

Let us consider again a general field function $b(\cdot,t,\mathbf{a})\in C^1(\mathcal{D})$ for all $t>t_0$ and all $\mathbf{a}$, Eq. (2.20) can be written as:

$$\partial_t f(x,t\mid\mathbf{a})+b(x,t,\mathbf{a})\partial_x f(x,t\mid\mathbf{a})=-f(x,t\mid\mathbf{a})\partial_x b(x,t,\mathbf{a}),\quad x\in\mathcal{D},\quad t>t_0, \tag{2.26}$$

and its solution can be analyzed through its characteristic equations [15,16,19]. These curves describe the time evolution of a particle, say $\phi(t)$, and the value of the desired PDE solution at that particle's position. These equations form a system of ODEs, which are defined as

$$\begin{aligned}\frac{\mathrm{d}}{\mathrm{d}t}\phi(t) &= b(\phi(t),t,\mathbf{a}), && \phi(0)=x_0,\\ \frac{\mathrm{d}}{\mathrm{d}t}f(\phi(t),t\mid\mathbf{a}) &= -f(\phi(t),t\mid\mathbf{a})\partial_x b(\phi(t),t,\mathbf{a}), && f(\phi(0),0\mid\mathbf{a})=f_0(x_0),\end{aligned} \tag{2.27}$$

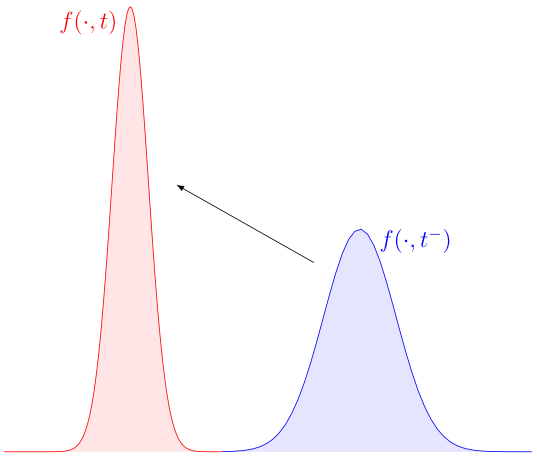

Fig. 2. PDF transformation at the impulse times. An illustrative example concerning the case of $\Gamma > 0$ almost surely.

where x_0 is a generic point in $\mathcal{D}$, which represents the initial position of the particle to be simulated. The first equation defines the time evolution of the particle's position, whereas the last equation in (2.27) defines the evolution of the PDF value in the considered particle.

Returning to our particular case, where $b(x,t) = g(x,t) - \sum_k \gamma_k \delta(t-t_k)x$, note that the field function $b(\cdot,t,\cdot) = g(\cdot,t,\cdot)$ for all $t \in \cup_{k=0}^{N-1}(t_k, t_{k+1})$. Therefore, between the impulse times, we can compute the solution of the Liouville equation by solving the characteristic Eqs. (2.27), in the corresponding intervals:

$$\phi(t;\, x_0, \mathbf{a}) = x_0 + \int_{t_k}^{t} g(\phi(s;\, x_0, \mathbf{a}), s, \mathbf{a})\mathrm{d}s, \quad t \in [t_k, t_{k+1}), \tag{2.28}$$

$$f(\phi(t;\, x_0, \mathbf{a}), t \mid \mathbf{a}) = f(x_0, t_k) \exp\left(-\int_{t_k}^{t} \partial_x g(\phi(s;\, x_0, \mathbf{a}), s, \mathbf{a})\mathrm{d}s\right), \quad t \in [t_k, t_{k+1}), \tag{2.29}$$

where $\phi(t;\, x_0, \mathbf{a})$ denotes the characteristic curve at time t, starting at (t_k, x_0), with parameter values $\mathbf{a}$. Note that, in Eq. (2.29), $f(\cdot, t_k)$ is obtained in Eq. (2.25).

As it can be seen, the first ODE in (2.27) and its corresponding solution (2.28) are the deterministic version of the random IVP (2.1) between impulses, solved for random samples x_0, and $\mathbf{a}$ of the initial condition $X_0(\omega)$ and parameter vector $\mathbf{A}(\omega)$, respectively, with $\omega \in \tilde{\Omega}$. The second equation in (2.27) and its solution (2.29) describe the change in the value of the PDF in time at the sample path $\phi(t;\, x_0, \mathbf{a})$.

2.2.3. Full evolution simulation

Summarizing, the PDF evolution of the random IVP (2.1) described by the Liouville equation can be split into the following steps:

(1) Define f_0, the PDF of the random initial condition $X_0(\omega)$.
(2) Compute its evolution for all realizations of the random parameter vector, $\mathbf{A}(\omega)$, via the characteristic Eqs. (2.27), until the first impulse time t_1. We now have a family of PDFs at time t_1 before the impulse, which we denote by $\{f(\cdot, t_1^- \mid \mathbf{a})\}_{\mathbf{a}\in\mathbf{A}(\Omega)}$.
(3) Compute the expected PDF with respect to the random parameter distribution, which we denote by $f(\cdot, t_1^-)$.
(4) Transform $f(\cdot, t_1^-)$ via (2.24), obtaining $f(\cdot, t_1)$.
(5) Repeat steps (1)–(4), but with $f_0(\cdot) = f(\cdot, t_1)$ until the following impulse time t_2.
(6) Repeat Steps (1)–(5) until the last impulse time, t_N using (2.25) and (2.27).
(7) Evolve $f(\cdot, t_N)$ until wanted.

The Liouville equation approach for the time evolution of the initial PDF f_0 is given as the solution to a PDE, whose solution is given by an ODE system, and the posterior substitution of its solution into another function whose form is known exactly. When a closed form of the sample path solution $\phi(t;\, x_0, \mathbf{a})$ is known, and we can solve for the initial condition variable (that is, if $x := \phi(t;\, x_0, \mathbf{a})$, then we can write $x_0(t;\, x, \mathbf{a})$), then the PDF is almost completely determined. All that is left is to compute the integral in (2.29), and the mean PDF with respect to the parameter distribution, which can be done analytically or numerically.

However, this approach is not always useful in general IVPs, where no closed-form expression of the solution is available. In that case, numerical methods might have to be used to obtain the characteristic curve $\phi(t;\, x_0)$ at certain

times. Regarding the case where no closed form expression of the solution $\phi(t;\, x_0)$ is available, the characteristic curve approach of the Liouville equation allows the use of the so-called Lagrangian methods [28,29], together with numerical techniques such as Adaptive Mesh Refinement (AMR) for the accurate and efficient computation of the PDF evolution.

3. Examples

This section is aimed at showing the applicability of the theoretical findings stated in the previous sections to some relevant random mathematical models where jumps are a key feature in the mathematical formulation. In [30,31], similar problems have been studied in the setting of the logistic equation, a classical and widely used mathematical model which appears in several areas of science. In this contribution, we are going to deal with the impulse-harvest generalized logistic model with a finite number of captures, say N,

$$\begin{aligned} X'(t,\omega) &= \alpha(t)\, r(\omega) X(t,\omega)\left(1-\left(\frac{X(t,\omega)}{K(\omega)}\right)^{\nu(\omega)}\right) - \sum_{n=1}^{N} \Gamma_n(\omega)\delta(t-t_n)X(t,\omega), \\ X(t_0,\omega) &= X_0(\omega), \end{aligned} \tag{3.1}$$

where $t \geq t_0$ and $\omega \in \tilde{\Omega}$. As usual, t is interpreted as the time, the parameter r is the growth ($r > 0$) or decay ($r < 0$) rate, and K is the carrying capacity. The differential equation is generalized by adding two terms: a positive, monotonically growing function $\alpha(\cdot)$ and a constant positive term ν. The first term, $\alpha(\cdot)$, allows controlling the so-called *lag phase*, which is the growth phase in which the population under study has not yet achieved fully exponential growth. In particular, we have chosen [32]:

$$\alpha(t) := \frac{q(\omega)}{q(\omega) + \mathrm{e}^{-m(\omega)\, t}}, \quad q, m > 0 \text{ a.s.}$$

The latter, ν, is a power that controls how fast the carrying capacity K is approached and is known as *deceleration* term. When $\nu = 1$, the classical logistic differential equation is obtained. And when ν tends to 0, the Gompertz equation is given. The incorporation of both the function $\alpha(\cdot)$ and the power ν allows for more flexible S-shaped curves to model growth phenomena over time.

We are going to simulate two examples with purely illustrative purposes. One will consider periodic impulses with non-identically, normally distributed intensities, while the second case will deal with periodic impulses with identically distributed intensities. In both cases the components of the parameter random vector $\mathbf{A}(\omega) = (q(\omega), m(\omega), r(\omega), K(\omega), \nu(\omega))$ will have appropriate pre-assigned parametric probability distributions. By no means the parameter values have been considered as an accurate representation of real-world behavior. They will only be considered so as to give a general idea about the capabilities to perform UQ for random differential equations with impulses.

The field function of the generalized logistic equation under study (3.1) verifies all the conditions of Theorem 2.1, where the set $\mathcal{D}$ in Theorem 2.1 for the generalized logistic model (3.1) is going to be $\mathcal{D} = [0, \|K\|_{\mathrm{L}^\infty}]$, with $\|K\|_{\mathrm{L}^\infty} = \sup\{K(\omega) : \omega \in \tilde{\Omega}\}$. Furthermore, it is smooth in space and time variables so the use of the Liouville equation as in (2.26) is available. Therefore, its corresponding Liouville equation between impulse times is:

$$\partial_t f(x,t \mid \mathbf{a}) + \alpha(t)\, rx\left(1-\left(\frac{x}{K}\right)^{\nu}\right)\partial_x f(x,t \mid \mathbf{a}) = -f(x,t \mid \mathbf{a})\alpha(t)\, r\left(1-(1+\nu)\left(\frac{x}{K}\right)^{\nu}\right).$$

We remind the computation of the marginal PDF respect to $\mathbf{A}$ as in Eq. (2.21). Using this final PDF, we will compute the statistical information given by the mean $\mathbb{E}[X(t,\omega)]$, and variance $\mathbb{V}[X(t,\omega)] = \mathbb{E}[(X(t,\omega))^2] - (\mathbb{E}[X(t,\omega)])^2$ at a certain prefixed time instant, say t.

3.1. Intravenous (I. V.) injections

Pharmacokinetics consists in the analysis and prediction of the concentration level of a certain drug inside an organism. It plays a key role when determining the appropriate levels and injection schedules that must be followed in order to achieve certain pre-established targets [33].

Drugs used for pain management are usually administered via I.V. injections. For example, morphine is a drug commonly used to treat severe pain due to cancer, surgery or trauma. However, a high dose of morphine is lethal [34]. Therefore, it is crucial to understand the dynamics of its concentration in the bloodstream before the actual administration schedule is chosen.

We can model this problem as (3.1), where the parameter vectors are chosen as follows:

- The initial drug concentration $X_0 \sim \mathrm{N}|_{(0,4)}(3.4, 0.025)$; that is, a normal distribution truncated on the interval $(0, 4)$.
- Variables q and m will be given the deterministic values $q = 1$ and $m = 4$.
- We consider $r \sim \mathrm{N}|_{(-1,0)}(-0.294, 0.025)$, $\nu \sim \mathrm{Unif}(1.1, 1.25)$ and $K \sim \mathrm{Unif}(3.9, 4)$.

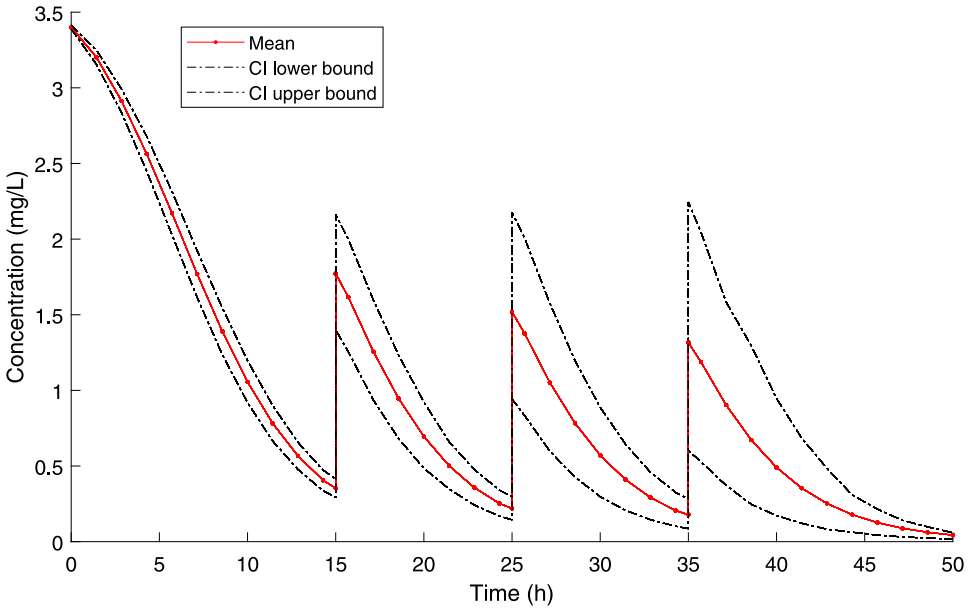

Fig. 3. Time evolution of the mean drug concentration and a 95% confidence interval with several injections.

- We are going to consider 3 injections, at times $T_{\text{IV}} = \{t_1 = 15, t_2 = 25, t_3 = 35\}$ (so $N = 3$), where the intensity of each injection will be given as

$$\Gamma_1 \sim \text{N}|_{(-1,0)}(-0.8, 0.01), \quad \Gamma_2 \sim \text{N}|_{(-1,0)}(-0.855, 0.01), \quad \Gamma_3 \sim \text{N}|_{(-1,0)}(-0.865, 0.01)$$

  As previously explained at the beginning of Section 2, the truncation interval has been chosen on the negative numbers so that the model correctly represents the absorption of the drug over time.

Fig. 3 shows the time evolution of the mean drug concentration as modeled by the generalized logistic Eq. (3.1) with the parameters chosen above. We can see that, after each injection, the uncertainty of the solution reflected by the amplitude of the 95%-confidence interval, suffers a great increase (see Fig. 4). This implies that no accurate predictions can be done for long-time concentrations with continued injections. However, the asymptotic state (or steady-state) is deterministic (the drug concentration converges to 0 asymptotically), and therefore, the uncertainty eventually reduces to 0 if no further injections are considered. Furthermore, Fig. 5 shows the full simulated PDFs computed as solutions of the Liouville equation for this specific problem. The PDFs after the jump are clearly seen as they are very wide, which is the sign of very high uncertainty in the system that can be seen in the other two Figs. 3 and 4.

3.2. Tumor removal

There are many ways of treating cancer, such as radiotherapy, chemotherapy, and in some cases, direct retrieval of a fraction of the tumor mass. The first two treatments have a prolonged effect of tumor destruction, whereas the latter intervention can be modeled via a delta-type impulse function because of the sudden extraction of the tumor mass with respect to the total treatment. Regarding un-altered tumor growth, it is well known that Malthus-type models of exponential growth only work when studying initial growth stages. Let us, therefore, model this problem as (3.1), where the parameter vectors are chosen as follows:

- The initial tumor size $X_0 \sim \text{N}|_{(0,1)}(0.15, 0.01)$, where $\text{N}|_{(0,1)}$ is a normal distribution truncated on the interval $(0, 1)$.
- Variables q and m will be given the same deterministic values as in the previous example: $q = 1$ and $m = 4$.
- We consider $r \sim \text{N}|_{(0,1)}(0.15, 0.0075)$, $\nu \sim \text{Unif}(1, 1.25)$ and $K \sim \text{Unif}(0.9, 1)$.
- We are going to consider 5 removals with equally distributed intensity given by $\Gamma_1 = \ldots = \Gamma_5 = \Gamma \sim \text{N}|_{\mathbb{R}^+}(2, 0.01)$, at times $T_{\text{Tumor}} = \{t_1 = 15, t_2 = 25, t_3 = 35, t_4 = 45, t_5 = 55\}$.

In Fig. 6, we have plotted the mean and 95%-confidence intervals according to the prefixed parameters and removal times. It can be seen how, after each removal, the tumor size starts growing according to the un-removed size of the tumor. Interestingly, the confidence interval amplitude before each removal is higher than the uncertainty after the removal. Indeed, since all removals are distributed as $\Gamma \sim \text{N}|_{\mathbb{R}^+}(2, 0.01)$, it can be easily seen that each removal takes away half of the tumor (in average), thus reducing the uncertainty after each removal time. Contrary to the previous example, this

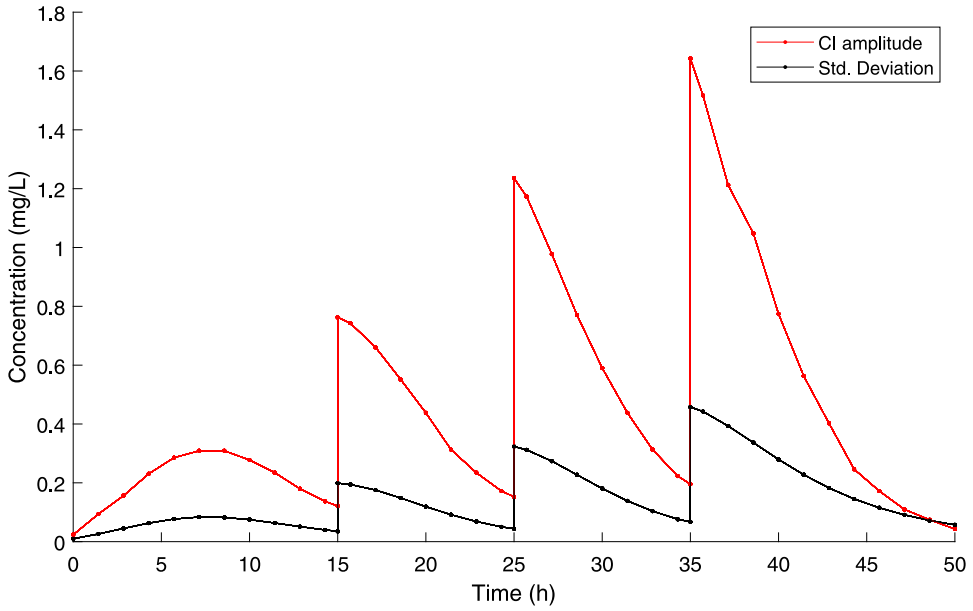

Fig. 4. Time evolution of the 95% Confidence Interval (CI) amplitude and the standard deviation of the drug concentration with repeated injections.

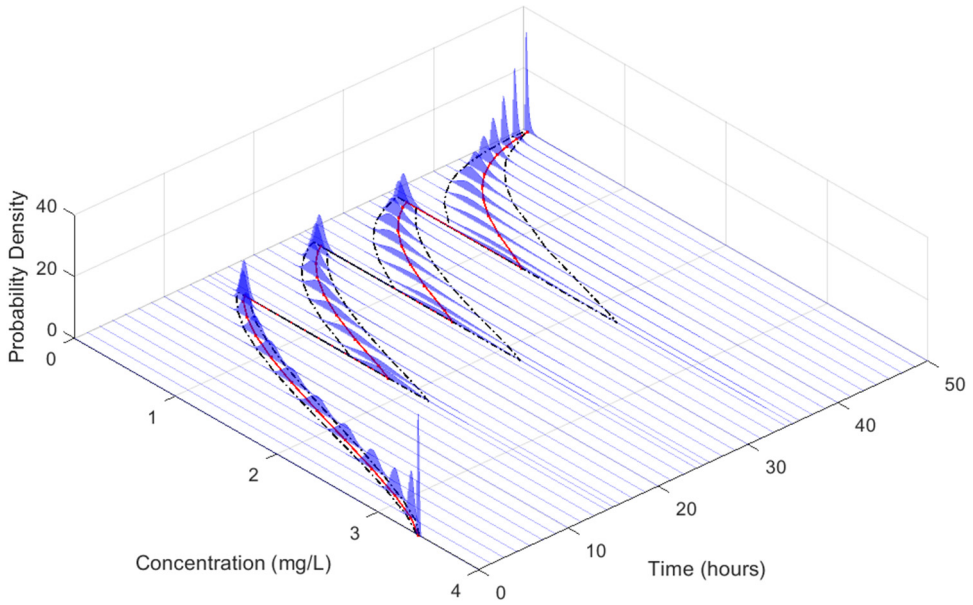

Fig. 5. Full view of the PDF evolution simulations of the I.V. Injection problem Section 3.1 at the corresponding time values in T_{IV} together with the mean (red) and 95% confidence interval (dashed, black). Compare to Fig. 3.

case allows having a long-time prediction with a reduced level of uncertainty while still considering random impulses (see Fig. 7). This can be further seen in Fig. 8, where the PDF given as the solution of the Liouville equation in this particular problem setting is shown in every simulated time in T_{Tumor}.

4. Conclusions and future work

In this contribution, we have rigorously obtained a pathwise solution to a general random differential equation with a finite number of random-intensity, state-dependent, impulsive terms, with the usual assumptions on the regularity of

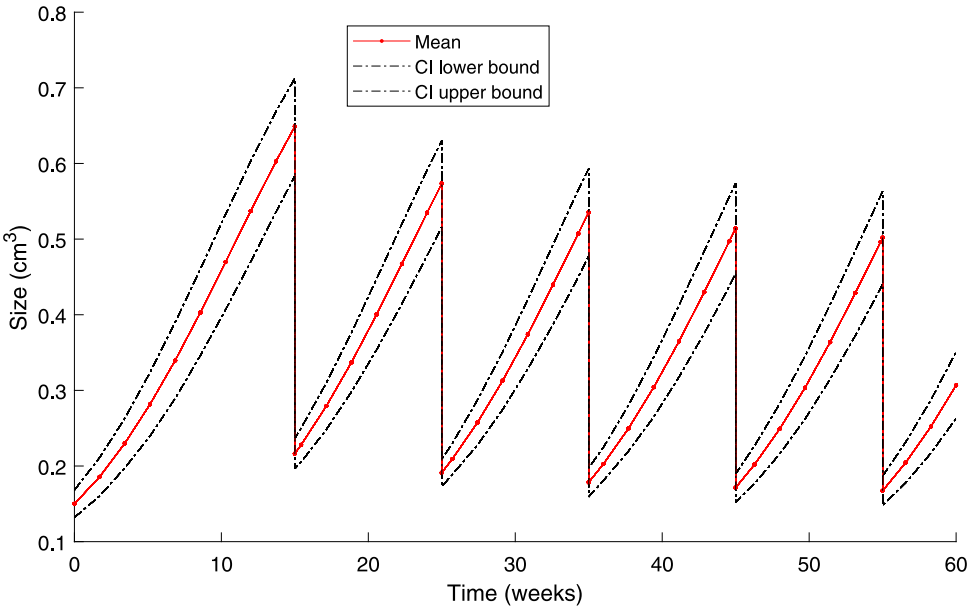

Fig. 6. Time evolution of the mean tumor size and a 95% confidence interval with several extractions.

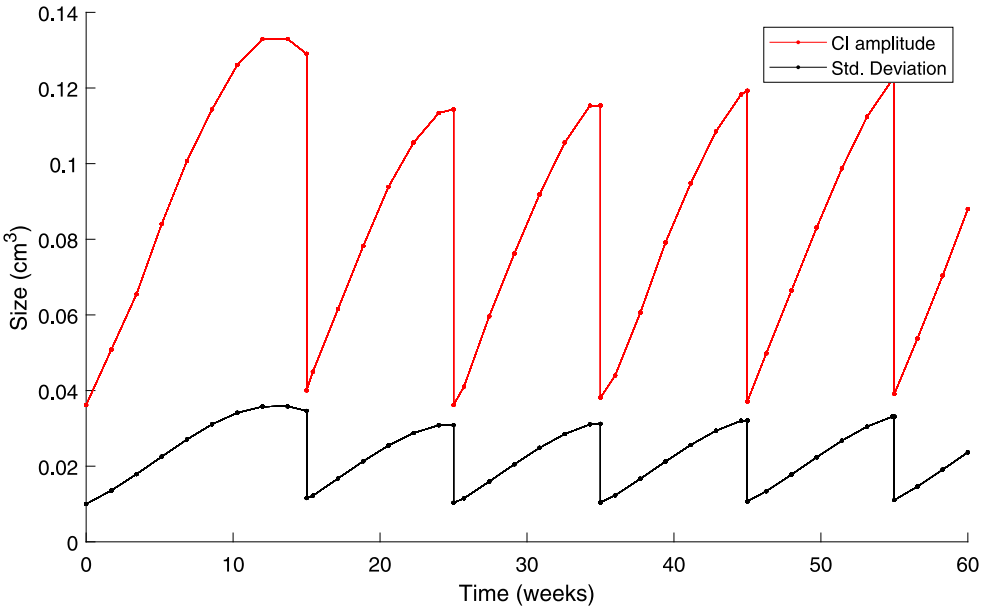

Fig. 7. Time evolution of the 95% Confidence Interval (CI) amplitude and the standard deviation of the tumor growth with extractions.

the field function. Furthermore, we have determined the evolution of the first probability density function of the solution stochastic process by combining the Liouville equation and the Random Variable Transformation theorem. After some brief comments on the numerical approach for the simulation of the probability density function evolution, we have applied our general theoretical findings to two mathematical models emerging from the generalized logistic model with natural decay and growth, respectively, being both altered by impulsive terms acting contrarily to their respective natural dynamics. This has been done to showcase the applicability of the theoretical findings in this contribution. Regarding future work, we are currently working on extending this approach to general Random Differential Systems and calibrating this family of models (Inverse Uncertainty Quantification) with respect to real data to model the behavior of a real-world system.

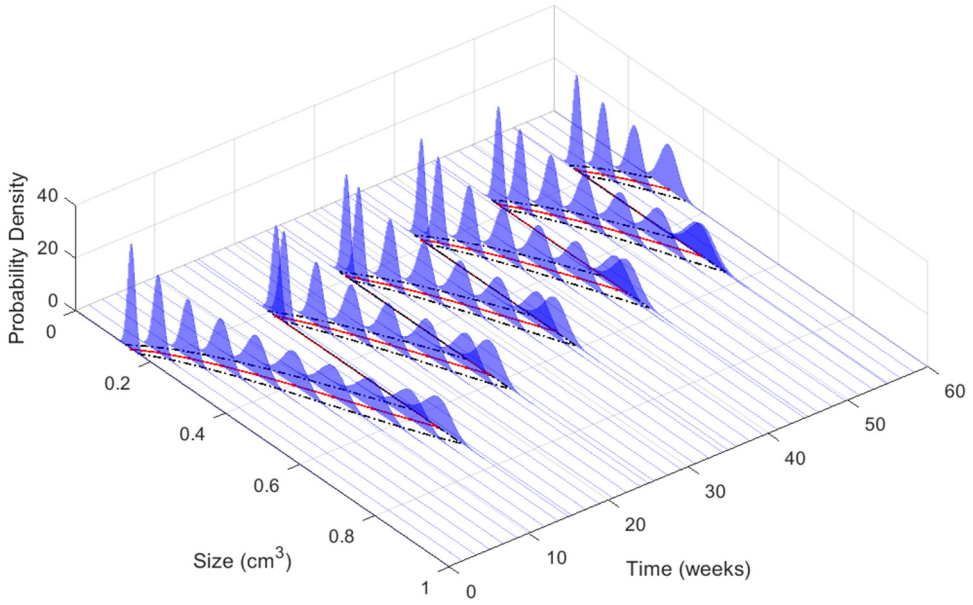

Fig. 8. Full view of the PDF evolution simulations of the tumor growth problem Section 3.2 at the corresponding time values in T_{Tumor}, together with the mean (red) and 95% confidence intervals (dashed, black). Compare with Fig. 6.

CRediT authorship contribution statement

Vicente J. Bevia: Conceptualization, Software, Formal analysis, Investigation, Writing – original draft, Writing – review & editing, Visualization. **Juan C. Cortés:** Conceptualization, Formal analysis, Investigation, Writing – original draft, Writing– review & editing, Supervision, Funding acquisition, Project administration. **Marc Jornet:** Conceptualization, Formal analysis, Investigation, Writing – original draft, Writing – review & editing. **Rafael J. Villanueva:** Conceptualization, Formal analysis, Investigation, Writing – original draft, Writing – review & editing, Supervision, Funding acquisition, Project administration.

Declaration of competing interest

The authors declare that they have no known competing financial interests or personal relationships that could have appeared to influence the work reported in this paper.

Data availability

No data was used for the research described in the article.

Acknowledgments

This work has been partially supported by the Spanish Ministerio de Economía, Industria *y* Competitividad (MINECO), the Agencia Estatal de Investigación (AEI), Spain, and Fondo Europeo de Desarrollo Regional (FEDER UE) grant PID2020–115270GB–I00, the Generalitat Valenciana, Spain (grant AICO/2021/302) and by el Fondo Social Europeo *y* la Iniciativa de Empleo Juvenil EDGJID/2021/185. Vicente Bevia acknowledges the doctorate scholarship granted by Programa de Ayudas de Investigación *y* Desarrollo (PAID), Universitat Politècnica de València, Spain.

References

[1] Zhang X, Shuai Z, Wang K. Optimal impulsive harvesting policy for single population. Nonlinear Anal RWA 2003;4(4):639–51. http://dx.doi.org/10.1016/S1468-1218(02)00084-6.
[2] Hritonenko N, Yatsenko Yu. Bang-bang, impulse, and sustainable harvesting in age-structured populations. J Biol Systems 2012;20(02):133–53. http://dx.doi.org/10.1142/S0218339012500088.
[3] Huang X, Yang B. Improving energy harvesting from impulsive excitations by a nonlinear tunable bistable energy harvester. Mech Syst Signal Process 2021;158:107797. http://dx.doi.org/10.1016/j.ymssp.2021.107797.
[4] Kiureghian A Der, Ditlevsen O. Aleatory or epistemic? Does it matter? Struct Saf 2009;31:105–12. http://dx.doi.org/10.1016/j.strusafe.2008.06.020.

[5] Smith Ralph C. Uncertainty quantification: theory, implementation and applications. Computational science and engineering, New York: SIAM; 2014.
[6] Xiu Dongbin. Numerical methods for stochastic computations: A spectral method approach. Computational science and engineering, New Jersey: Princeton University Press; 2010.
[7] Soong TT. Random differential equations in science and engineering. New York: Academic Press; 1973.
[8] Kroese DP, Brereton TJ, Taimre T, Botev ZI. Why the Monte Carlo method is so important today. Wiley Interdiscip Rev Comput Stat 2014;6.
[9] Caflisch RE. Monte Carlo and quasi-Monte Carlo methods. Acta Numer 1998;7:1–49. http://dx.doi.org/10.1017/S0962492900002804.
[10] Morokoff WJ, Caflisch RE. Quasi-Monte Carlo Integration. J Comput Phys 1995;122(2):218–30. http://dx.doi.org/10.1006/jcph.1995.1209.
[11] Jornet M, Calatayud J, Maître Olivier P Le, Cortés JC. Variance reduction methods and multilevel Monte Carlo strategy for estimating densities of solutions to random second-order linear differential equations. Int J Uncertain Quantif 2020;10(5):467–97. http://dx.doi.org/10.1615/Int.J.UncertaintyQuantification.2020032659.
[12] Dorini FA, Cecconello MS, Dorini LB. On the logistic equation subject to uncertainties in the environmental carrying capacity and initial population density. Commun Nonlinear Sci Numer Simul 2016;33:160–73. http://dx.doi.org/10.1016/j.cnsns.2015.09.009.
[13] Slama H, Hussein A, El-Bedwhey NA, Selim MM. An approximate probabilistic solution of a random SIR-type epidemiological model using RVT technique. Appl Math Comput 2019;361:144–56. http://dx.doi.org/10.1016/j.amc.2019.05.019.
[14] Bevia V, Burgos C, Cortés JC, Navarro-Quiles A, Villanueva R-J. Uncertainty quantification analysis of the biological Gompertz model subject to random fluctuations in all its parameters. Chaos Solitons Fractals 2020;138:109908. http://dx.doi.org/10.1016/j.chaos.2020.109908.
[15] Bevia V, Burgos C, Cortés JC, Navarro A, Villanueva RJ. Analysing differential equations with uncertainties via the Liouville-Gibbs theorem: Theory and applications. In: Zeidan D, Padhi S, Burqan A, Ueberholz P, editors. Computational mathematics and applications. Singapore: Springer Singapore; 2020, p. 1–23. http://dx.doi.org/10.1007/978-981-15-8498-5_1.
[16] Bevia V, Burgos C, Cortés JC, Villanueva RJ. Uncertainty quantification of random microbial growth in a competitive environment via probability density functions. Fractal Fract 2021;5(2). http://dx.doi.org/10.3390/fractalfract5020026.
[17] Santambrogio F. Optimal transport for applied mathematicians. calculus of variations, PDEs and modeling. Birkhäuser Cham; 2015, http://dx.doi.org/10.1007/978-3-319-20828-2.
[18] Villani C. Optimal transport: Old and new. Heidelberg: Springer Berlin; 2008, http://dx.doi.org/10.1007/978-3-540-71050-9.
[19] Evans LC. Partial differential equations. Providence, R.I.: American Mathematical Society; 2010, ISBN: 978-1-4704-6942-9.
[20] Jornet M. Liouville's equations for random systems. Stoch Anal Appl 2021;1–22. http://dx.doi.org/10.1080/07362994.2021.1980015.
[21] Hermoso A, Homar V, Yano JI. Exploring the limits of ensemble forecasting via solutions of the Liouville equation for realistic geophysical models. Atmos Res 2020;246:105127. http://dx.doi.org/10.1016/j.atmosres.2020.105127.
[22] Loève M. Probability theory I. New York: Springer New York, NY; 1977.
[23] Gasquet C, Witomski P. Fourier analysis and applications. filtering, numerical computation, wavelets. Springer; 1998.
[24] Teschl G. Ordinary differential equations and dynamical systems. American Mathematical Society; 2012.
[25] Peano J. Démonstration de l'intégrabilité des équations différentielles ordinaires. Math Ann 1890;37:182–228.
[26] Dyke P. An introduction to Laplace transforms and Fourier series. Springer London; 2014.
[27] Benedetto John J. Harmonic analysis and applications. CRC Press; 1997.
[28] Batchelor GK. An introduction to fluid dynamics. Cambridge University Press; 1973.
[29] Bergdorf M, Koumoutsakos P. A Lagrangian Particle-Wavelet Method. Multiscale Model Simul 2006;5(3):980–95. http://dx.doi.org/10.1137/060652877.
[30] Cortés JC, Delgadillo-Alemán S, Ku-Carrillo R, Villanueva RJ. Probabilistic analysis of a class of impulsive linear random differential equations forced by stochastic processes admitting Karhunen-Loève expansions. Discrete Contin Dyn Syst - S 2022. http://dx.doi.org/10.3934/dcdss.2022079.
[31] Cortés JC, Moscardó-García A, Villanueva RJ. Uncertainty quantification for hybrid random logistic models with harvesting via density functions. Chaos Solitons Fractals 2022;155:111762. http://dx.doi.org/10.1016/j.chaos.2021.111762.
[32] Ram Y, Dellus-Gur E, Bibi M, Karkare K, Obolski U, Feldman MW, Cooper TF, Berman J, Hadany L. Predicting microbial growth in a mixed culture from growth curve data. Proc Natl Acad Sci 2019;116(29):14698–707. http://dx.doi.org/10.1073/pnas.1902217116.
[33] Buclin T, Nicod M, Kellenberger S. Pharmacokinetics: Online content for student, https://sepia2.unil.ch/pharmacology/. [Accessed: 16 June 2022].
[34] Boyer EW. Management of opioid analgesic overdose. N Engl J Med 2012;367(2):146–55. http://dx.doi.org/10.1056/NEJMra1202561.